# $\alpha$ clusters and collective flow in ultra-relativistic carbon–heavy nucleus collisions

Piotr Bożek,[1,2,*] Wojciech Broniowski,[3,2,†] Enrique Ruiz Arriola,[4,‡] and Maciej Rybczyński[3,§]

[1] *AGH University of Science and Technology, Faculty of Physics and Applied Computer Science, al. Mickiewicza 30, 30-059 Krakow, Poland*
[2] *The H. Niewodniczański Institute of Nuclear Physics, Polish Academy of Sciences, PL-31342 Cracow, Poland*
[3] *Institute of Physics, Jan Kochanowski University, 25-406 Kielce, Poland*
[4] *Departamento de Física Atómica, Molecular y Nuclear and Instituto Carlos I de Física Teórica y Computacional, Universidad de Granada, E-18071 Granada, Spain*

We investigate ultrarelativistic collisions of the $^{12}$C nucleus with heavy targets and show that the harmonic flow measures based on ratios of cumulant moments are particularly suited to study the intrinsic deformation of the $^{12}$C wave function. That way one can probe the expected $\alpha$ clusterization in the ground state, which leads to large initial triangularity in the shape of the fireball in the transverse plane. We show that the clusterization effect results in very characteristic behavior of the ratios of the cumulant moments as functions of the number of participant nucleons, both for the elliptic and triangular deformations. Thus the experimental event-by-event studies of harmonic flow in ultrarelativistic light-heavy collisions may offer a new window to look at the ground-state structure of light nuclei.

PACS numbers: 21.60.Gx, 25.75.Ld

arXiv:1410.7434v1 [nucl-th] 27 Oct 2014

## I. INTRODUCTION

In a recent paper [1] a novel method of investigating the $\alpha$ clusterization of light nuclei was proposed, exploring an unexpected bridge between the lowest-energy nuclear physics determining the ground-state structure and the highest-energy nuclear collisions. In this work we further pursue the method of searching for specific signals of the intrinsic geometry of light nuclei manifest in harmonic flow. Our approach is based on the fact that at the ultra-high collision energies, where the nucleon-nucleon inelastic collisions generate a stream of copious particles, the interaction times are short enough to prevent the much slower nuclear excitations. Therefore, the initial spatial distributions of nucleons in the nuclear ground state of the overlaying nuclei mark the location of sources (inelastic collisions) igniting the fireball.

Atomic nuclei have a genuine degree of granularity which can be characterized by typical correlation lengths and which reflects the energetically favored spatial orderings. Any such geometric feature should leave some fingerprint in the final state, provided these effects and the random fluctuations due to finite number of particles can be cleanly separated. The theoretical identification and the experimental verification of these geometry-preserving features would provide not only valuable information on conventional nuclear structure, where genuine multi-nucleon aspects of the nuclear wave functions could be tested, but would also generate confidence on the currently intricate theoretical protocols and the approximation schemes used to analyze the dynamics of relativistic heavy-ion collisions.

In this paper we analyze in further detail the possible experimental signatures of presence of the $\alpha$ clusters in $^{12}$C, which is of direct significance for analysis of its ultrarelativistic collisions with a heavy target. In particular, we focus on the ratios of harmonic flow measures investigated in the hydrodynamic framework [2] for the case of the $^3$He-Au collisions and defined in a suitable way such that the sensitivity to the details of the intermediate dynamical/collective stages of the fireball evolution is eliminated. Such careful procedures are needed, as the studied observables carry information on both the initial geometry of the fireball, as well as on its random fluctuations which have the tendency of covering up the geometry to some extent.

We show that the intrinsic triangular geometry of $^{12}$C, predetermined by the arrangement of the $\alpha$ clusters, leads to very specific and pronounced dependence of the considered measures on the number of nucleons participating in the collision. We argue that the proposed method provides practical tools to investigate signatures of the cluster structure of the ground-state wave function of light nuclei, and that it could be directly employed in studies of future ultrarelativistic heavy-ion collisions of light-heavy systems.

The paper, designed for both the researchers of the $\alpha$-clusterization and the relativistic heavy-ion community, is arranged as follows: In Sec. II A we briefly review the current status of the $\alpha$ clusterization in light nuclei, in the scope needed for our work. Based on that knowledge we prepare our nuclear Monte Carlo configurations of $^{12}$C as described in Sec. II B. These configurations are later used in the simulations of collisions with a heavy target.

Then we pass to presenting our modeling of the early stage of the collision, stressing its quantum-mechanical

* Piotr.Bozek@ifj.edu.pl
† Wojciech.Broniowski@ifj.edu.pl
‡ earriola@ugr.es
§ Maciej.Rybczynski@ujk.edu.pl

aspects in Sec. III A. The important point here is that the reaction time at ultrarelativistic energies is much shorter from any typical nuclear-dynamics time, resulting in a frozen configuration of the nucleons reflecting the structure of the ground-state nuclear wave function. The formation of the fireball is described in Sec. III B, where we apply the popular Glauber approach [3–8] for our event-by-event studies. The key quantities here are the eccentricity parameters, defined in Sec. III C.

In Sec. IV A we turn to harmonic flow – phenomenon used extensively in the relativistic heavy-ion programs to infer properties of the dynamically evolving quark-gluon plasma with the help of well-developed methods [9–12]. From our point of view, the essential feature here is the approximately linear response of the dynamical system to the eccentric deformation of the initial state, resulting in proportionality of the measurable flow coefficients to the corresponding initial eccentricity parameters. The unknown response coefficient may be eliminated by taking appropriate ratios of moments of the distribution, as explained in Sec. IV B. In particular, we consider moments based on the two- and four-particle cumulants, used frequently in experimental studies. Such ratios for the flow moments are equal to the corresponding ratios of the eccentricity moments, thus allowing for predictions of the measured quantities related to flow based solely on measures of the initial state. Moreover, these ratios are sensitive to the geometry and random fluctuations in a very specific way.

In particular, we find that for the $^{12}$C collisions on a heavy target, the ratio of the four- to two-particle cumulant moments changes behavior for the high-multiplicity events (centrality below 10%), increasing with the number of participating nucleons for triangularity, and decreasing for ellipticity, in accordance with the geometric features of the system. This is the key result of this work.

The feature holds at various collision energies (Sec. V A) and rapidities (Sec. V B), as well as for different Glauber models of the initial state (Sec. V D. We have also checked the dependence of our results on the model of the $^{12}$C wave function (Sec. V D).

## II. $\alpha$ CLUSTERS IN LIGHT NUCLEI

### A. Overview

The idea of $\alpha$ clustering dates back to the old work of Gamow [13], where he conceived the radioactive $\alpha$-decay process as a signal for nuclear constituents. This is in agreement with the tight binding ($B_\alpha/4 \sim 7$ MeV), and compactness ($r_\alpha \sim 1.5$fm) of the quartet of states ($p\uparrow$, $p\downarrow$, $n\uparrow$, $n\downarrow$) building the $^4$He nucleus and the weak $\alpha\alpha$ attraction ($V_{\alpha\alpha} \sim -2.5$MeV) gluing the $\alpha$-particles into the light $A = 4n$ nucleus [14–16] (see, e.g., [17] for an early review and [18] for a historic account). This has been one of the most fascinating issues of the nuclear structure physics throughout decades (for reviews of the topic see, e.g., [19–25]).

The $^{12}$C nucleus is of particular interest. It was described as a bound state of three elementary $\alpha-$particles by Harrington [26] (for a review and further references see [27]). Numerous theoretical approaches were applied to its ground-state and excited states structure: the Bose-Einstein Condensation (BEC) model [28], the fermionic molecular dynamics (FMD) [29], antisymmetrized molecular dynamics [30], effective chiral field theory on the lattice [31], the no-core shell model [32, 33], or the variational Green's function method (VMC) [34]. The recently discovered $5^-$ rotational state of $^{12}$C in low energy $\alpha+^{12}$C collisions points to the triangular $\mathcal{D}_{3h}$ symmetry of the system [35].

### B. Generating clustered distributions

Our aim is to consider $\alpha$-clustered ground-state structure of $^{12}$C. Ideally, distributions following from realistic model wave functions or ab initio calculations should be used. As this is quite involved, or requires access to the Monte Carlo nuclear configurations in the path-integral Green's function methods, we proceed in a simplified manner which grasps the essential features of the ground-state distributions and serves our purpose to sufficient accuracy. As we wish to study the effects of clusterization, we assume that $^{12}$C is formed of three separated $\alpha$ clusters. The parameters of the arrangement are adjusted in such a way that the desired one-body radial density of the centers of nucleons is reproduced, as described below.

Technically, we carry out the Monte Carlo simulations of the nuclear configurations as follows: we place the centers of the three clusters in an equilateral triangle of edge length $l$. The distribution in each cluster is a Gaussian parametrized as

$$f_i(\vec{r}) = A \exp\left(-\frac{3}{2}\,(\vec{r}-\vec{c_i})^2/r_\alpha^2\right), \tag{1}$$

where $\vec{r}$ is the coordinate of the nucleon, $\vec{c_i}$ is the position of the center of the cluster $i$, and $r_\alpha$ is the rms radius of the cluster. We generate randomly the positions of the nucleons, in sequence alternating the number of the cluster: 1, 2, 3, 1, 2, 3, etc., and taking into account the short-distance NN repulsion in a popular way, where the centers of each pair of nucleons cannot be closer than 0.9 fm [37]. At the end of the procedure the distributions are shifted such that their center of mass is placed at the origin of the coordinate frame. As a result, we get the Monte Carlo $^{12}$C distributions with the built-in $\alpha$-cluster correlations.

The model parameters $l$ and $r_\alpha$ are optimized in such a way that the desired form of the radial density is obtained. Thus the radial density of the centers on nucleons serves as a constraint for building the clustered distributions. Throughout this paper we use two reference radial distributions: those obtained from the so-

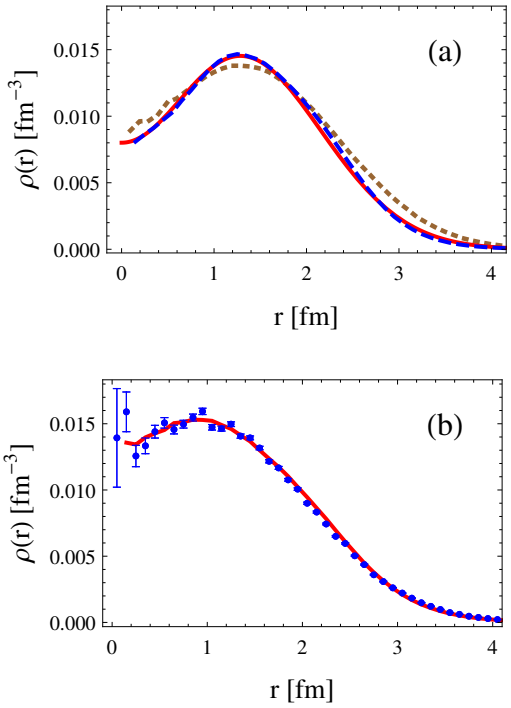


FIG. 1. (Color online) (a) Radial distribution of the centers of nucleons in $^{12}C$ for the BEC calculation reproducing the charge form factor (dashed line), our parametrization of the BEC calculation (solid line), and the Jastrow calculation of Ref. [36] (dotted line). (b) The VMC calculation (points) and our parametrization (solid line). See text for details.

TABLE I. Parameters used in our Monte Carlo simulations for the distributions of nucleons in $^{12}$C.

| parameter | BEC | VMC |
|---|---|---|
| $l$ [fm] | 3.05 | 2.84 |
| $r_\alpha$ [fm] | 0.96 | 1.15 |

called Bose-Einstein Condensation (BEC) model [28] and distributions from the variational Monte Carlo calculations (VMC) using the Argonne v18 two-nucleon and Urbana X three-nucleon potentials, as recently provided in `http://www.phy.anl.gov/theory/research/density`. Figure 1 shows the quality of our fit to the one-body densities for the two considered cases: BEC in Fig. 1(a) and VMC in Fig. 1(b), where we also give for a reference the result of the Jastrow-type correlated wave function [38].

The parameters used in our simulations are collected in Table I. As $l$ is much larger than $r_\alpha$, the distributions are hollow in the center, and the curves in Fig. 1 exhibit a dip, more depleted as $r_\alpha/l$ decreases. We note that, after properly implementing the nucleon charge contribution with $r_N = 0.87$fm, the BEC densities reproduce very well the charge form factor of $^{12}$C, which is not the case of VMC, albeit the charge density near the origin carries rather large uncertainties inherited from the lack of knowledge in the high-momentum region in the measured charge form factor. As the BEC case is more strongly clustered than the VMC case ($r_\alpha/l$ is smaller), we shall use it as our basic model to illustrate the investigated effects, which are stronger with this choice. We will occasionally compare also to the VMC scenario.

As we are interested in specific effects of clusterization, as a "null result" we also use the *uniform* distributions, i.e., with no $\alpha$ clusters. We prepare such distributions with exactly the same radial density as the clustered ones. This is achieved easily with a trick, where we randomly regenerate the spherical angles of the nucleons from the clustered distributions, while leaving the radial coordinate intact.

While the above-described procedure may seem crude for the description of the nuclear structure, it is sufficient for our goal. We note that the method reproduces not only the one-body densities, as shown above, but also the two-particle densities determined from multicluster models with the state-dependent Jastrow correlations [38] are describes with a reasonable accuracy ($\sim 10-20\%$) [39] .

## III. EARLY-STAGE OF THE ULTRA-RELATIVISTIC REACTION

### A. Quantum-mechanical aspects of the collision

Viewed in the lab frame of collider experiments, the colliding ultra-relativistic nuclei move almost with the speed of light. The corresponding Lorentz contraction factors are very large (∼1000 at the LHC and ∼100 at the RHIC energies), such that we deal with collisions of "flat pancakes" and hence the initial-state interactions are negligible; the reaction time is much shorter than any typical and slow nuclear structure time scale to witness any relevant nuclear excitation. As a result, in the reaction, a frozen nuclear ground-state configuration is seen. The wave function undergoes quantum-mechanical reduction in the earliest stage of the reaction, which results in a given intrinsic nuclear configuration. As outlined above, we generate event-by-event probability following the square of the nucleus wave function.

The heavy nucleus which collides with $^{12}$C (here $^{197}$Au or $^{208}$Pb) is made according to the Monte Carlo procedure described in detail [40, 41]. The short-distance NN repulsion and the nuclear deformation effects are taken into account.

Note that since $^{12}$C is much smaller than $^{197}$Au or $^{208}$Pb, for sufficiently small impact parameters the collisions correspond to the $\alpha$-clustered, triangle-shaped, and randomly oriented nucleus bumping into the central region of a heavy nucleus. This can pictorially be idealized as an equilateral triangle of three-$\alpha$'s *hitting a wall* of nuclear matter.

In the following we are concerned with the transverse plane, relevant for the mid-rapidity physics studied later, hence we only need the wave functions in the transverse plane and mid-rapidity. The typical locations of the centers of $^{12}$C nucleons are indicated with small diamonds

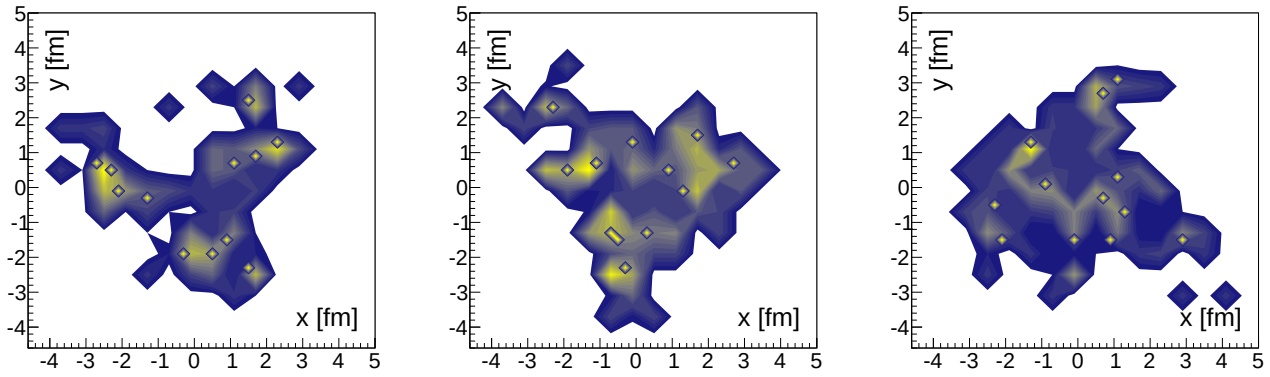


FIG. 2. (Color online) Snapshots of three sample $^{12}$C–$^{197}$Au events, displaying the distribution of sources in the transverse plane. The small diamonds indicate the positions of the $^{12}$C nucleons, while the dark region shows the density of the fireball including the wounded nucleons from $^{197}$Au and the binary collisions. BEC case, RHIC, $N_{\rm w} = 66$. In this simulation the transverse and cluster planes were aligned for better visualization. See text for details.

in Fig. 2.

### B. Formation of the fireball

The initial density of the fireball in ultra-relativistic heavy-ion collisions is formed out of the individual NN collisions between nucleons from the two colliding nuclei. At these high energies most collisions are inelastic and copious particles (partons) are produced. Popular modeling of this phase is accomplished with the Glauber approach [3–8], applied in this work. One may alternatively adopt the Kharzeev-Levin-Nardi framework [42–44] based on the Color Glass Condensate model which rests explicitly on quark-gluon dynamics (see, e.g., [45]).

Within the Glauber framework, we use the so-called mixed model [42, 46], where the entropy deposition in the transverse plane comes from the wounded nucleons [5], defined as those who interacted inelastically at least once, and from the binary collisions. A source coming from the wounded nucleon is placed in its center with a relative weight $(1-a)/2$, while the location of the binary collision is in the center of mass of the colliding nucleon pair, while the relative weight is $a$. The probability of the collision is defined relative to the total inelastic NN cross section, $\sigma_{\rm NN}^{\rm inel}$, corresponding to the CM collision energy in the process. The NN collision profile corresponds to the probability of an NN inelastic collision to happen at a given impact parameter $b$. We use the smooth function described in [40, 41], which is constructed to reproduce approximately the differential elastic NN cross section. The values of parameters used in our simulations are listed in Table II.

The Monte Carlo simulation produces, in each event, the location of the centers of the sources distributed in the transverse plane. Physically, sources generated in a collision process are of non-zero width, reflecting the production mechanism (non-zero size of nucleons, flux tubes, etc.) and thus the sources must be *smeared*. This feature can be modeled by placing a two-dimensional Gaussian of width $\sigma$ (in this paper we take $\sigma = 0.4$ fm) centered at the source in the transverse plane. This *physical* smearing effect is necessary in forming the initial condition for hydrodynamics, taking over the evolution of the system. Also, smearing is phenomenologically important for the shape eccentricities, which are significantly reduced compared to the naive evaluation with point-like sources. This smearing length sets a typical coarse graining scale for hydrodynamics beyond which the integration step would not explore the relevant physics.

TABLE II. Parameters used in the GLISSANDO simulations.

| | system | $\sqrt{s_{\rm NN}}$ [GeV] | $\sigma_{\rm NN}^{\rm inel}$ [mb] | $a$ |
|---|---|---|---|---|
| SPS | $^{12}$C+$^{208}$Pb | 17 | 32 | 0.12 |
| RHIC | $^{12}$C+$^{197}$Au | 200 | 42 | 0.145 |
| LHC | $^{12}$C+$^{208}$Pb | 5200 | 73 | 0.15 |

Sample events of central $^{12}$C–$^{197}$Au collision are presented in Fig. 2. We have used here the clustered $^{12}$C BEC distributions and, for the purpose of better visibility, aligned the transverse and the cluster planes (the carbon hits the lead "flat"). The small diamonds mark the positions of the $^{12}$C nucleons, while the dark region represents the transverse density of the fireball, including the wounded nucleons from $^{197}$Au and the binary collisions. The irregular "warped" structure follows from the stochastic nature of the process. Nevertheless, one may easily notice the remnant triangular shape in the fireball distribution, originating from the underlying three $\alpha$ clusters in $^{12}$C.

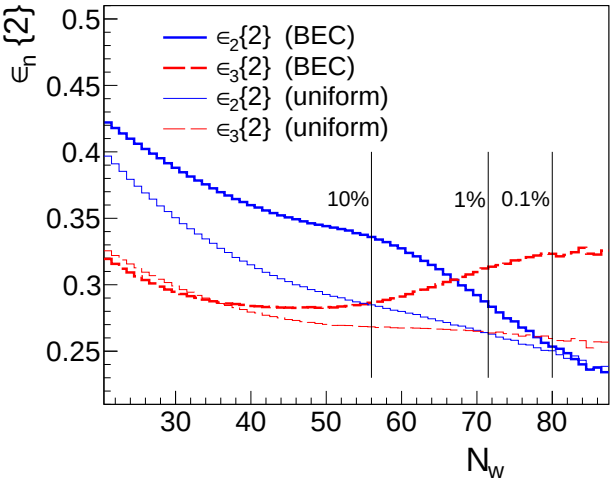


FIG. 3. (Color online) Comparison of the fireball eccentricity coefficients from the two-particle cumulants for the clustered distribution and for the uniform distribution. GLISSANDO simulations, BEC case, RHIC. The vertical lines indicate total number of the wounded nucleons corresponding to centralities 10%, 1% and 0.1%. The orientation-multiplicity correlation is clearly seen for the clustered case.

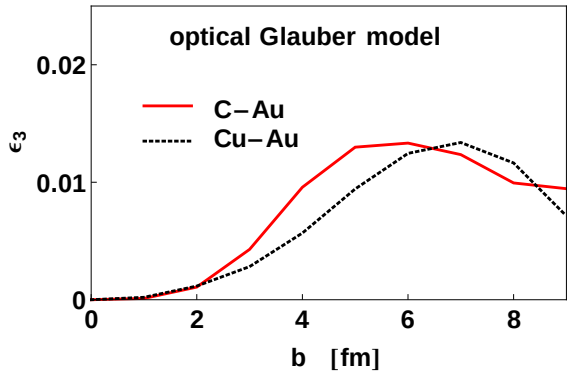


FIG. 4. (Color online) Triangularity of the fireball formed in C-Au and Cu-Au collisions. The density is calculated in the optical Glauber model, and the the triangularity is defined with respect to the reaction plane.

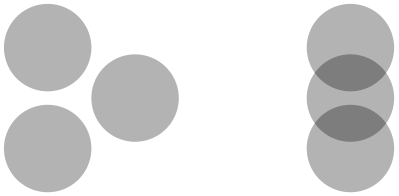

FIG. 5. (Color online) The flat-on (left) and side-wise (right) orientations of $^{12}$C with respect to the reaction plane.

### C. Eccentricities of the initial state

With the smeared sources, the eccentricity parameters of the fireball, $\epsilon_n$, are defined in each event via the Fourier decomposition of the density in the transverse plane,

$$\epsilon_n e^{in\Phi_n} = -\frac{\int dxdy\, f(x,y)\rho^n e^{in\phi}}{\int dxdy\, f(x,y)\rho^n}, \qquad (2)$$

where $n = 2, 3, \ldots$ is the rank, $\Phi_n$ is the angle of the principal axes, $x$ and $y$ are coordinates in the transverse plane, with $\rho = \sqrt{x^2+y^2}$ and $\tan\phi = y/x$, finally, $f(x,y)$ is the fireball density in the given event. The $n = 2$ eccentricity is termed *ellipticity*, and $n = 3$ *triangularity*.

Non-vanishing contributions to the coefficients $\epsilon_n$ come from two different origins. One of them is the intrinsic "geometry" of the distribution of the nucleons in $^{12}$C. In the clustered case there is a large triangularity of this distribution from the arrangement of the $\alpha$ clusters in an equilateral triangle. Although it is somewhat reduced due to random orientation of the $^{12}$C nucleus with respect to the transverse plane, the values of $\epsilon_3$ remain sizable. The $^{12}$C nucleus also exhibits geometric ellipticity in the case when the cluster plane is not parallel to the transverse plane, which is the generic case due to randomness of the orientation.

The second cause for eccentricity coefficients comes from fluctuations due to the finite number of nucleons [7, 47–50]. The effect of fluctuations washes away to some extent the geometric component, hence a careful examination of the results presented in Sec. IV B is necessary to discriminate the two different origins.

In collisions of asymmetric nuclei at a finite impact parameter $b$, small values of odd Fourier components can appear in the azimuthal dependence of the fireball density with respect to the reaction plane (such an effect is present, for instance, in the Cu-Au collisions). In Fig. 4 we show the triangularity of the initial fireball for the C-Au and Cu-Au collisions with respect to the reaction plane calculated in the optical Glauber model, an approximate scheme where one first averages the densities and then computes the nuclear thickness function [51]. For intermediate values of $b$ the triangularity is non-zero, even without any contribution from fluctuations or the $\alpha$ clustering. However, the obtained value of $\epsilon_3$ is an order of magnitude smaller than the one calculated event-by-event with respect to the third order event plane (Fig. 3). Moreover, the most central collisions that we discuss in the following correspond to small impact parameters (for centralities $c = 10\%$, 1% and 0.1% the average values of $b$ are 2.4, 1.5, and 1.2 fm, respectively). Hence the average geometric $\epsilon_3$ in the reaction plane is even smaller. While the above effect is automatically included in our simulation, it does not play a role in the interpretation of the results.

As already explained in [1], there is a specific correlation between centrality, triangularity, and ellipticity, induced by the intrinsic orientation of $^{12}$C. When the transverse and the cluster planes are aligned, the $^{12}$C nucleus hits the large nucleus flat-on and thus creates most damage, i.e., produces the largest number of sources (cf. left

side of Fig. 5). At the same time, in this flat-on orientation we have on the average the highest triangularity and the lowest ellipticity, which here comes entirely from fluctuations.

In the other extreme case the cluster plane is perpendicular to the transverse plane (side-wise configuration, cf. right side of Fig. 5). Then we find the opposite behavior: low multiplicity, as the cross section is smaller, small triangularity, and large ellipticity, which now obtains a sizable contribution from the elongated shape of the fireball.

Of course, in actual collisions the orientation is random and we have a situation between the two limiting cases described above, yet the phenomenon of the specific orientation-multiplicity correlations is clearly seen (cf. top-right Fig. 3 of Ref. [1] or Fig. 3 in this paper). In particular, in Fig. 3 we see, by comparing the simulations with clustered and uniform $^{12}$C, that the geometry raises triangularity at high values of the number of wounded nucleons, $N_w$ (preferentially flat-on collisions), and raises ellipticity at lower values of $N_w$ (side-wise collisions).

Event-by-event studies allow for obtaining event-by-event distributions of the physical quantities. In the Sections below we will need the so-called two-particle and four-particle cumulants moments [52] of the eccentricities, defined as

$$\epsilon_n\{2\} = \langle\epsilon_2^2\rangle^{1/2},$$
$$\epsilon_n\{4\} = 2\left(\langle\epsilon_n^2\rangle^2 - \langle\epsilon_n^4\rangle\right)^{1/4}. \qquad (3)$$

For a finite number of sources (wounded nucleons), even without geometric deformation, one has just from fluctuations $\epsilon_n\{m\} \neq 0$ for $m \geq 4$, with $\epsilon_n\{m\}$ decreasing as $1/N_w^{1-1/m}$ [50, 53].

## IV. COLLECTIVITY AND DEVELOPMENT OF HARMONIC FLOW

### A. Flow coefficients

The eccentricity coefficients described in the previous Section are not directly observable, as they correspond to the stage right after one nucleus impinges on the other. In a hydrodynamic approach this is just the initial stage, whereas what one measures are the harmonic flow coefficients $v_n$, defined as the Fourier coefficients of the azimuthal dependence of the particle spectra, namely

$$\frac{dN}{d\phi} = \frac{N}{2\pi}\left[1 + 2\sum_n v_n \cos\left[n(\phi - \Psi_n)\right]\right] \qquad (4)$$

(here we consider the $v_n$ coefficients integrated over the transverse momentum).

Realistic modeling of the flow coefficients requires advanced simulations of all stages of the reaction, from the early phase, through the intermediate hydrodynamics (for reviews see, e.g., [54, 55] and references therein) or transport [56], to hadronization at freeze-out (see, e.g., [51] for a review). Such event-by-event simulations have been carried out for numerous reactions, displaying collectivity even for such small system as in d-Au and p-Pb collisions [57–62].

A crucial finding for our method is that to a very good accuracy the flow coefficients are proportional to the ini-

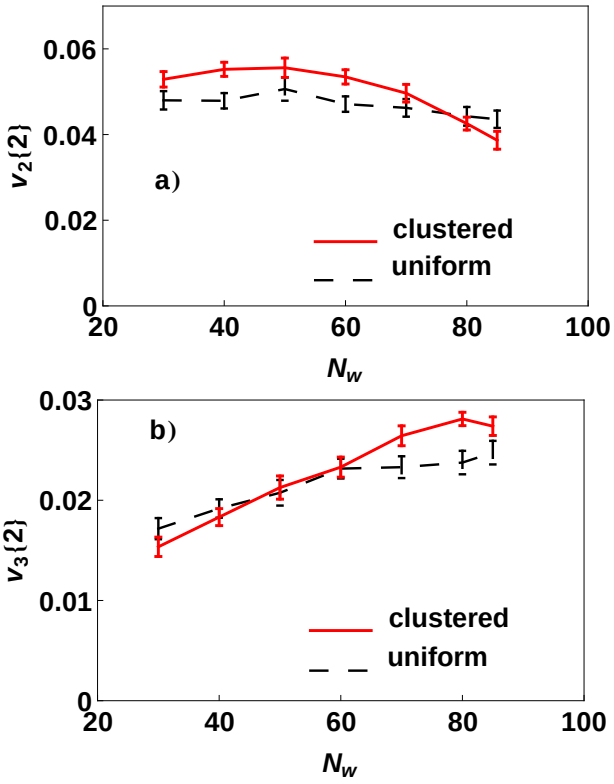


FIG. 6. (Color online) Elliptic (panel a) and triangular (panel b) flow coefficients as a function of the number of wounded nucleons for C-Au collisions, calculated using the second order cumulant.

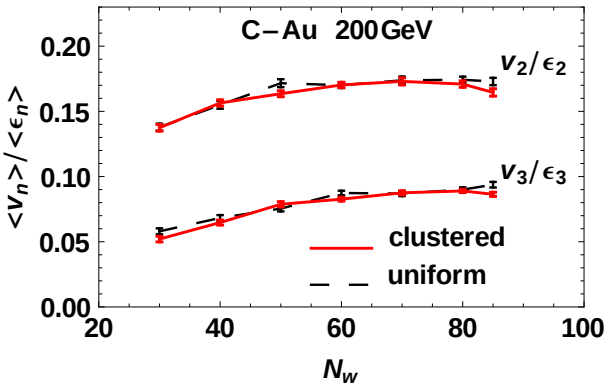


FIG. 7. (Color online) The hydrodynamic response coefficients for ellipticity and triangularity plotted as functions of the total number of wounded nucleons. BEC case, RHIC, 3+1 dimensional viscous hydrodynamics.

tial eccentricity coefficients [63, 64],

$$v_n = \kappa_n \epsilon_n, \quad n = 2, 3. \tag{5}$$

The response coefficients $\kappa_n$ depend on the details of the system and model (collision energy, multiplicity, viscosity of quark-gluon plasma, initial time of collective evolution, freeze-out temperature, feature of the applied "afterburner"), yet the linearity of Eq. (5) allows for model-independent studies for certain quantities as shown in the following Sections. These relations, realizing the shape-flow transmutation phenomenon, buttress quantitatively the naive expectation of geometry-preserving features addressed in the introduction.

We have carried out hydrodynamic simulations for the studied case of $^{12}$C-$^{197}$Au collisions at RHIC energies. We have used the event-by-event 3+1 dimensional viscous hydrodynamics of Ref. [65]. At the freeze-out temperature of 150 MeV hadrons are emitted following the statistical hadronization model [66, 67]. The hydrodynamic evolution and particle emission at freeze-out include effects of the shear viscosity with $\eta/s = 0.08$ and the bulk viscosity with $\zeta = 0.04$ [68]. In Fig. 6 we present the obtained estimates for the elliptic $v_2\{2\}$ and triangular $v_3\{2\}$ (all charged hadrons, 150 MeV$< p_\perp < 2$ GeV, $|\eta| < 1$) flow coefficients for two cases: the clustered and the uniform initial $^{12}$C configurations. It is not possible to obtain directly accurate estimates of the higher-order cumulants $v_n\{4\}$ or $v_n\{6\}$ due to prohibitive requirements on the event-by-event statistics.

Our simulations confirm the approximate linearity of Eq. 5. The resulting response coefficients are presented in Fig. 7. We note that the response coefficients grow with $N_w$. The relative growth is quite strong, in particular $\kappa_3$ increases by 50% from $N_w = 30$ to $N_w = 80$.

### B. Ratios of flow coefficients

The above-mentioned increase of the response coefficient with multiplicity poses an obstacle in qualitative analyses of the clusterization effect. Imagine that the experiment finds a growth of triangularity with $N_w$. A priori, without a detail knowledge of the structure of the initial state and details of the dynamics, we cannot say how much of this growth should be attributed to intrinsic geometric deformation, and how much comes from the enhanced hydrodynamic response. One may avoid this difficulty by taking ratios of moments of event-by-event distributions of $\epsilon_n$ which are independent of $\kappa_n$. Thanks to the proportionality (5), the same relations hold for the moments of $v_n$. Two popular choices with the low-order moments are the scaled standard deviation

$$\frac{\sigma(\epsilon_n)}{\langle \epsilon_n \rangle} \simeq \frac{\sigma(v_n)}{\langle v_n \rangle}, \tag{6}$$

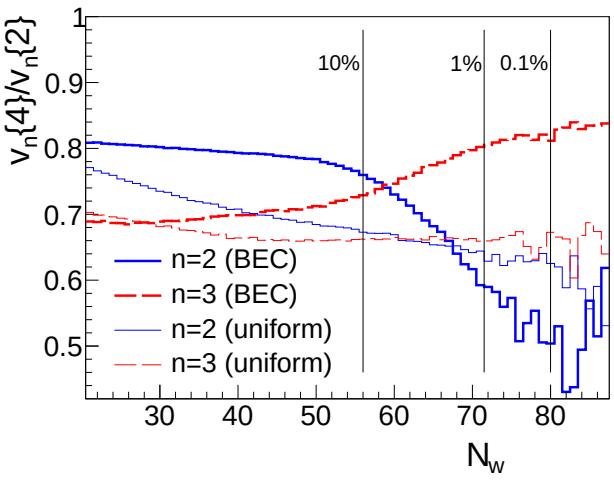


FIG. 8. (Color online) Ratios of four-particle to two-particle cumulants plotted as functions of the total number of wounded nucleons. BEC case, RHIC.

and the ratio of the four-particle and two-particle cumulant moments,

$$\frac{\epsilon_n\{4\}}{\epsilon_n\{2\}} \simeq \frac{v_n\{4\}}{v_n\{2\}}. \tag{7}$$

Thus measurements of the above combinations of moments of $v_n$ provide information on analogous quantities for the eccentricities. Experimentally, one can access even moments of $v_n$, and the ratio in Eq. (6) must be estimated from $v_n\{2\}$ and $v_n\{4\}$ or from the reconstructed $v_n$ distribution.

Predictions based on Eq. (6) may be found already in Ref. [1] (top-right Fig. 3 in that work), where $\sigma(\epsilon_n)/\langle \epsilon_n \rangle$ grows for ellipticity and decreases for triangularity with $N_w$. This behavior reflects the interplay of the intrinsic geometry and statistical fluctuations. In this paper, following closely the analysis of Ref. [2], we apply relation (7). The results of GLISSANDO simulations are shown in Fig. 8. We note that for high multiplicity collisions the ratio $\epsilon_n\{4\}/\epsilon_n\{2\}$ significantly grows for triangularity and decreases for ellipticity. The geometric triangularity increases for collisions with a larger number of participants, corresponding to high multiplicity events. On the other hand, the eccentricity due to fluctuations of independent sources decreases with $N_w$, hence the opposite behavior.

We note that the change of behavior (stronger monotonicity) starts at $N_w$ corresponding to centrality of 10%, thus occurs in the region easily accessible to experimental analyses. We also see that the behavior for the clustered $^{12}$C (thick lines in Fig. 8) is completely different from the case of the uniform structure (thin lines).

The behavior shown in Fig. 8 is the key result of this work. It offers a signature sensitive to the intrinsic deformation that is straightforward to measure in ultra-

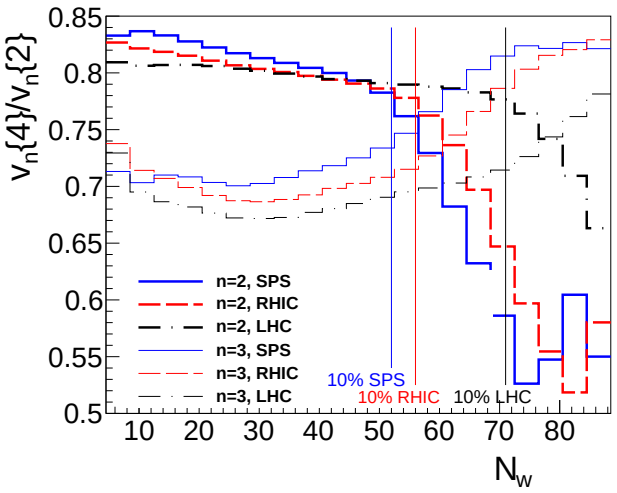


FIG. 9. (Color online) Comparison of $v_n\{4\}/v_n\{2\}$ for the SPS, RHIC, and LHC cases. BEC case. The vertical lines indicate the values of $N_w$ corresponding to centralities 10% for the three collision energies. Parameters are listed in Table II.

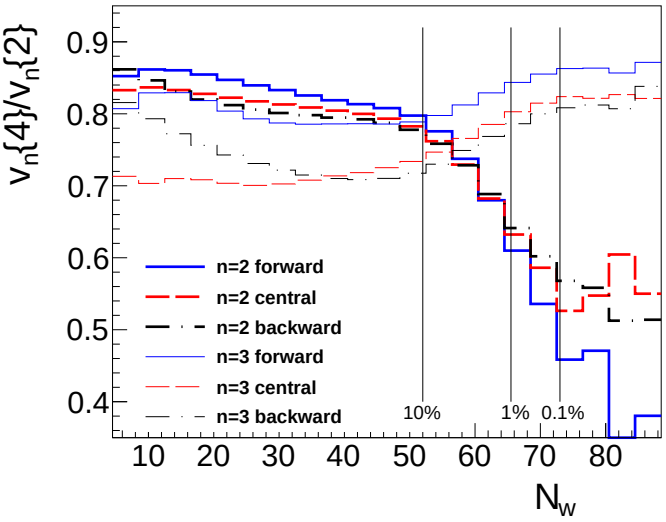


FIG. 10. (Color online) Ratios of the four-particle to two-particle cumulants in forward, central, and backward rapidity regions, plotted as functions of the total number of the wounded nucleons. BEC case, SPS.

relativistic heavy-ion collisions with standard techniques devoted to analysis of harmonic flow.

One could ask at this point why we do need to resort to Eq. (7), rather than evaluate $v_n\{4\}$ directly from the event-by-event hydrodynamic calculations. The reason is two-fold. First, the statistics possible to achieve in such studies is sufficient for the analysis of two-particle cumulants, but not four-particle cumulants. Secondly, and more importantly, the application of Eq. (7) frees us from sensitivity to details of the dynamical theory, which we do not know exactly. That way the predictions for the ratios of the cumulant moments are more general and model-independent.

## V. FURTHER RESULTS

### A. Dependence on the collision energy

In Fig. 9 we show the dependence of our predictions on the collision energy, according to the values in Table II. We note that the qualitative predictions do not change with the collision energy, as the three sets of curves are similar, in particular when we take into account the fact that the values of centrality corresponding to a given $N_w$ depend on the energy via the value of $\sigma_{\rm NN}^{\rm inel}$.

### B. Forward and backward rapidity

We may also ask the question on how much the predictions depend on the rapidity window used in the experiment. This is of practical significance, as in fixed-target experiments the detectors cover rapidity away from the center. For the purpose of a simple estimate, we use the model of Refs. [69, 70], where the initial density of the fireball in the space-time rapidity $\eta_\parallel$ and the transverse plane coordinates $(x, y)$ is given by the form

$$F(\eta_\parallel, x, y) = (1-a)[\rho_+(x,y)f_+(\eta_\parallel) + \rho_-(x,y)f_-(\eta_\parallel)] + a\rho_{\rm bin}(x,y)\left[f_+(\eta_\parallel) + f_-(\eta_\parallel)\right], \quad (8)$$

where $\rho_\pm(x, y)$ is the density from the forward- and backward-going wounded nucleons, $\rho_{\rm bin}(x, y)$ is the binary collisions density. The rapidity profile functions $f_+(\eta_\parallel)$ and $f_-(\eta_\parallel)$ are given explicitly in Ref. [70].

For our purpose it only matters that at mid-rapidity $f_\pm(0) = 1/2$, hence $F(0) = (1-a)\frac{1}{2}(\rho_+ + \rho_-) + a\rho_{\rm bin}$, which is nothing else but the density of the mixed model used up to now to evaluate the fireball eccentricities. At very forward rapidities $\eta_+$ the value of $f_-(\eta_+)$ is negligible compared to $f_+(\eta_+)$, hence the relevant density of the fireball is $F(\eta_+) = f_+(\eta_+)\,[(1-a)\rho_+ + a\rho_{\rm bin}]$. Analogously, at large backward rapidities $\eta_-$ we have $F(\eta_-) = f_-(\eta_-)\,[(1-a)\rho_- + a\rho_{\rm bin}]$.

The results of the calculation using central, forward (i.e., the $^{12}$C hemisphere), and backward rapidity windows, with the source density constructed according to the above-described prescription, is shown in Fig. 10. We note that the results do not alter much with the choice of rapidity. We can see that the forward case has the largest ratio for the triangularity, which follows from the fact that it is more sensitive to the distribution of nucleons in the clustered $^{12}$C. However, the monotonic behavior is not very different, and there should not be much differ-

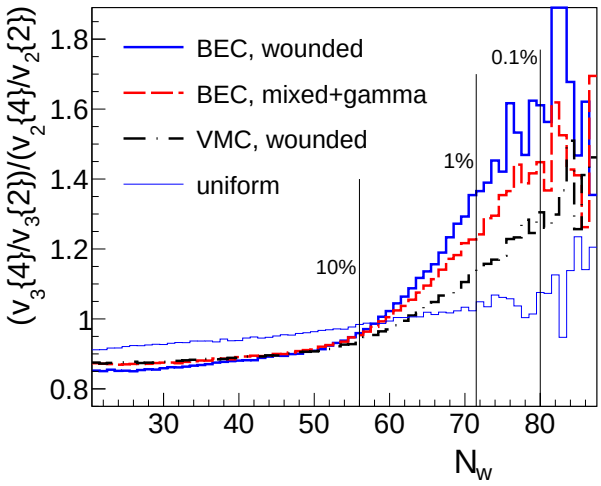


FIG. 11. (Color online) Comparison of the double ratio $(v_3\{4\}/v_3\{2\})/(v_2\{4\}/v_2\{2\})$ for various models, plotted as functions of the total number of wounded nucleons, RHIC.

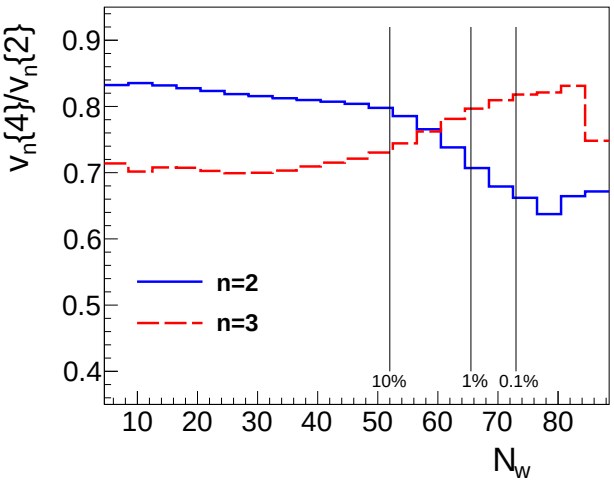


FIG. 12. (Color online) Predictions for $v_n\{4\}/v_n\{2\}$ for the $^{12}$C distribution where the $\alpha$ clusters are arranged in a deformed triangle mimicking the FMD calculation of Ref. [29]. SPS case. See text for details.

ence in the results obtained at mid-rapidity in colliders and peripheral rapidity in fixed-target experiments.

### C. Dependence on the model of the initial state

Up to now we have used the mixed model of the formation of the initial state, and the BEC distribution in $^{12}$C. In this subsection we study other variants of the Glauber approach, as well as the VMC distributions. The studied effects of clusterization depends to some extent on the models of the initial state, as they involve different amount of fluctuation. They also obviously depend on the configuration of the ground state of $^{12}$C. In Fig. 11 we present the double ratio $(v_3\{4\}/v_3\{2\})/(v_2\{4\}/v_2\{2\})$ for several cases.

We notice the difference between the wounded nucleon model (less fluctuations) and the mixed model with the overlaid gamma distribution [40] (significantly more fluctuations). On the other hand, the result for the VMC distributions is, as expected from the discussion of Sec. II B, significantly weaker. Such a sensitivity is desired, as it in principle allows for a quantitative discrimination of the $^{12}$C wave functions from the studies of flow in ultrarelativistic collisions.

### D. Deformed triangle

Finally, we study the case where the $^{12}$C nucleus is formed by placing the three $\alpha$ clusters in a deformed isosceles triangle, as results from the Fermionic Molecular Dynamics (FMD) studies of Ref. [29]. For that purpose we take the ratio of the length of the edges to be 3/4, the value that can be read off from the right-most plot in Fig. 2 of Ref. [29].

The results of this calculation displayed in Fig. 12 show that the qualitative behavior is the same as for the case of the equilateral triangle studied in the preceding sections.

## VI. CONCLUSIONS

We have pursued the idea that there is a geometry preserving principle operating in ultrarelativistic collisions, involving light nuclei impinging on heavy ions. The extremely high energies make the interaction time so short that the existing granular structures present in the ground-state nuclear wave function are effectively frozen. The collision process realizes a snapshot which may be recorded as a pattern in the collective flow emerging from the abundantly produced particles in individual nucleon-nucleon inelastic collisions.

The presence of fluctuations due to the finite number of particles as well the limitations imposed by the finite nuclear size cause the geometric signals to be generically blurred by random fluctuations. For that reason a careful analysis, as described in this paper, must be carried out.

We have addressed the question of intrinsic triangularity structure of $^{12}$C motivated by the ancient idea that it has a cluster structure with the three $\alpha$-particles sitting in the corners of an equilateral triangle and the fact that the 12 nucleons induce a sufficiently large collectivity when colliding with heavy ions such as $^{197}$Au or $^{208}$Pb. Other light isotopes in the region $A \sim 10$ may undergo a similar study as the one conducted here.

Furthermore, our analysis is insensitive to the hydrodynamic details by relying on the linear response of the

harmonic flow to the initial conditions. For that purpose, we examine the ratios of cumulant moments, which are very well suited for our strategy. We find that visible signals are expected in the dependence of these ratios on the number of wounded nucleons, a feature which makes them particularly suitable for experimental analysis.

The fascinating possibility of catching the $^{12}C$ nucleus as a triangle of $\alpha$ particles in ultrarelativistic collisions would provide further evidence of Gamow's idea, taken from a different angle as traditionally expected, and could be discerned on experimental grounds. A positive answer would also generate further confidence on the currently intricate theoretical approaches.

## ACKNOWLEDGMENTS

This research was supported by by the Polish National Science Centre, grants DEC-2011/01/D/ST2/00772 and DEC-2012/06/A/ST2/00390, Spanish DGI (grant FIS2011-24149) and Junta de Andalucía (grant FQM225), and PL-Grid infrastructure.

[1] W. Broniowski and E. Ruiz Arriola, Phys.Rev.Lett. **112**, 112501 (2014)
[2] P. Bożek and W. Broniowski(2014), arXiv:1409.2160 [nucl-th]
[3] R. J. Glauber in *Lectures in Theoretical Physics* W. E. Brittin and L. G. Dunham eds., (Interscience, New York, 1959) Vol. 1, p. 315
[4] W. Czyż and L. Maximon, Annals Phys. **52**, 59 (1969)
[5] A. Białas, M. Błeszyński, and W. Czyż, Nucl.Phys. **B111**, 461 (1976)
[6] M. L. Miller, K. Reygers, S. J. Sanders, and P. Steinberg, Ann.Rev.Nucl.Part.Sci. **57**, 205 (2007)
[7] W. Broniowski, P. Bożek, and M. Rybczyński, Phys.Rev. **C76**, 054905 (2007)
[8] A. Białas, J.Phys. **G35**, 044053 (2008)
[9] J.-Y. Ollitrault, Phys.Rev. **D46**, 229 (1992)
[10] N. Borghini, P. M. Dinh, and J.-Y. Ollitrault, Phys.Rev. **C64**, 054901 (2001)
[11] S. Voloshin, Nucl.Phys. **A715**, 379 (2003)
[12] S. A. Voloshin, A. M. Poskanzer, and R. Snellings(2008), arXiv:0809.2949 [nucl-ex]
[13] G. Gamow, *Constitution of atomic nuclei and radioactivity* (Oxford University Press, 1931)
[14] J. A. Wheeler, Phys.Rev. **52**, 1083 (1937)
[15] L. R. Hafstad and E. Teller, Phys. Rev. **54**, 681 (1938)
[16] W. Wefelmeier, Zeitschrift für Physik **107**, 332 (1937)
[17] J. Blatt and V. Weisskopf, *Theoretical nuclear physics* (New York: John Wiley and Sons, 1952)
[18] D. Brink, in *Journal of Physics: Conference Series*, Vol. 111 (IOP Publishing, 2008) p. 012001
[19] D. Brink, Proc. Int. School Enrico Fermi, Course **36** (1965)
[20] M. Freer, Reports on Progress in Physics **70**, 2149 (2007)
[21] K. Ikeda, T. Myo, K. Kato, and H. Toki, *Clusters in Nuclei-Vol.1* (Lecture Notes in Physics **818**, Springer, 2010)
[22] C. Beck, *Clusters in Nuclei-Vol.2* (Lecture Notes in Physics **848**, Springer, 2012)
[23] J. Okołowicz, W. Nazarewicz, and M. Płoszajczak, Fortsch.Phys. **61**, 66 (2013)
[24] P. I. Zarubin, *Clusters in Nuclei-Vol.3* (Springer, 2014)
[25] C. Beck(2014), arXiv:1408.0684 [nucl-ex]
[26] D. R. Harrington, Phys.Rev. **147**, 685 (1966)
[27] M. Freer and H. Fynbo, Prog.Part.Nucl.Phys. **78**, 1 (2014)
[28] Y. Funaki, A. Tohsaki, H. Horiuchi, P. Schuck, and G. Röpke, Eur.Phys.J. **A28**, 259 (2006)
[29] M. Chernykh, H. Feldmeier, T. Neff, P. von Neumann-Cosel, and A. Richter, Phys.Rev.Lett. **98**, 032501 (2007)
[30] Y. Kanada-En'yo, Prog.Theor.Phys. **117**, 655 (2007)
[31] E. Epelbaum, H. Krebs, T. A. Lahde, D. Lee, and U.-G. Meissner, Phys.Rev.Lett. **109**, 252501 (2012)
[32] R. Roth, S. Binder, K. Vobig, A. Calci, J. Langhammer, *et al.*, Phys.Rev.Lett. **109**, 052501 (2012)
[33] B. R. Barrett, P. Navratil, and J. P. Vary, Prog.Part.Nucl.Phys. **69**, 131 (2013)
[34] S. C. Pieper, K. Varga, and R. B. Wiringa, Phys.Rev. **C66**, 044310 (2002)
[35] D. Marin-Lambarri, R. Bijker, M. Freer, M. Gai, T. Kokalova, *et al.*, Phys.Rev.Lett. **113**, 012502 (2014)
[36] E. Buendía, F. Gálvez, J. Praena, and A. Sarsa, J. Phys. **G27**, 2211 (2001)
[37] W. Broniowski and M. Rybczyński, Phys.Rev. **C81**, 064909 (2010)
[38] E. Buendia, F. Galvez, and A. Sarsa, Phys.Rev. **C70**, 054315 (2004)
[39] W. Broniowski and E. Ruiz Arriola(2014), arXiv:1407.8495 [nucl-th]
[40] W. Broniowski, M. Rybczyński, and P. Bożek, Comput.Phys.Commun. **180**, 69 (2009)
[41] M. Rybczyński, G. Stefanek, W. Broniowski, and P. Bożek, Comput.Phys.Commun. **185**, 1759 (2014)
[42] D. Kharzeev and M. Nardi, Phys.Lett. **B507**, 121 (2001)
[43] D. Kharzeev, E. Levin, and M. Nardi, Nucl.Phys. **A730**, 448 (2004)
[44] H.-J. Drescher, A. Dumitru, A. Hayashigaki, and Y. Nara, Phys.Rev. **C74**, 044905 (2006)
[45] J. L. Albacete and C. Marquet, Prog.Part.Nucl.Phys. **76**, 1 (2014)
[46] B. Back *et al.* (PHOBOS Collaboration), Phys.Rev. **C65**, 031901 (2002)
[47] M. Miller and R. Snellings(2003), arXiv:nucl-ex/0312008 [nucl-ex]
[48] S. Manly *et al.* (PHOBOS Collaboration), Nucl.Phys. **A774**, 523 (2006)
[49] S. A. Voloshin(2006), arXiv:nucl-th/0606022 [nucl-th]
[50] B. Alver and G. Roland, Phys.Rev. **C81**, 054905 (2010)
[51] W. Florkowski, *Phenomenology of Ultra-Relativistic Heavy-Ion Collisions* (World Scientific Publishing Company, Singapore, 2010)
[52] N. Borghini, P. M. Dinh, and J.-Y. Ollitrault, Phys.Rev. **C63**, 054906 (2001)

[53] R. S. Bhalerao and J.-Y. Ollitrault, Phys.Lett. **B641**, 260 (2006)
[54] U. Heinz and R. Snellings, Ann.Rev.Nucl.Part.Sci. **63**, 123 (2013)
[55] C. Gale, S. Jeon, and B. Schenke, Int.J.Mod.Phys. **A28**, 1340011 (2013)
[56] Z.-W. Lin, C. M. Ko, B.-A. Li, B. Zhang, and S. Pal, Phys.Rev. **C72**, 064901 (2005)
[57] P. Bożek, Phys.Rev. **C85**, 014911 (2012)
[58] A. Adare *et al.* (PHENIX Collaboration), Phys.Rev.Lett. **111**, 212301 (2013)
[59] A. M. Sickles (PHENIX Collaboration)(2013), arXiv:1310.4388 [nucl-ex]
[60] P. Bożek, W. Broniowski, and G. Torrieri, Phys.Rev.Lett. **111**, 172303 (2013)
[61] A. Bzdak, B. Schenke, P. Tribedy, and R. Venugopalan, Phys.Rev. **C87**, 064906 (2013)
[62] G.-Y. Qin and B. Müller, Phys.Rev. **C89**, 044902 (2014)
[63] F. G. Gardim, F. Grassi, M. Luzum, and J.-Y. Ollitrault, Phys.Rev. **C85**, 024908 (2012)
[64] H. Niemi, G. Denicol, H. Holopainen, and P. Huovinen, Phys.Rev. **C87**, 054901 (2013)
[65] P. Bożek, Phys.Rev. **C85**, 034901 (2012)
[66] A. Kisiel, T. Tałuć, W. Broniowski, and W. Florkowski, Comput.Phys.Commun. **174**, 669 (2006)
[67] M. Chojnacki, A. Kisiel, W. Florkowski, and W. Broniowski, Comput.Phys.Commun. **183**, 746 (2012)
[68] P. Bożek, Phys.Rev. **C81**, 034909 (2010)
[69] A. Białas and W. Czyż, Acta Phys.Polon. **B36**, 905 (2005)
[70] P. Bożek and I. Wyskiel, Phys.Rev. **C81**, 054902 (2010)